PHYSICAL REVIEW B VOLUME 31, NUMBER 4 15 FEBRUARY 1985

Effects of polysilane formation on the optical and electrical properties of binary Si:H alloys

Shoji Furukawa and Nobuo Matsumoto
Musashino Electrical Communication Laboratory, Nippon Telegraph and Telephone Public Corporation, Musashino-shi, Tokyo 180, Japan
(Received 11 July 1984)

Wide-optical-gap (up to 2.4 eV) binary Si:H alloys containing many polysilane $(SiH_2)_n$ groups were prepared by rf glow discharge and disilane. Optical band gaps increased monotonically with a decrease in the substrate temperature T_s during deposition in the range $440 \gtrsim T_s \gtrsim 220$ K. The increase in the optical band gap is closely related to the infrared-absorption strength for a $\sim$845-cm^{-1} peak, which is due to $(SiH_2)_n$ wagging vibrations. The infrared-absorption wave number for all peaks is increased slightly with an increase in polysilane formation. The shift in infrared-absorption wave number is explained by the electronegativity difference due to $(SiH_2)_n$-group formation. The polysilane-chain length n can be estimated by the stretching wave-number shift, and is evaluated as $n \sim 11$ for an alloy prepared at $T_s \sim 300$ K. The binding energies of Si inner electrons and the ESR spin density do not show a monotonical change with a change in T_s, but show a critical change at around 360 K. This T_s value corresponds to $n = 1$—2, or the temperature below which $(SiH_2)_n$ ($n \geq 2$) groups are formed. Both photoconductivity and photoluminescence spectra suggest the existence of broad tail states in wide-optical-gap alloys.

I. INTRODUCTION

The physical properties of binary Si:H alloys depend greatly on both the incorporated hydrogen content and the Si—H bond configuration. At the highest hydrogen-content limit that can be realized by a polysilane $(SiH_2)_n$ structure for Si:H alloys, the physical properties are expected to be greatly different from those of conventional hydrogenated amorphous silicon (*a*-Si:H). Moreover, it can be said that linear chained polysilanes are potential precursors to one-dimensional semiconductors. Up to the present, three methods have been presented for polysilane preparation. One is the chemical method, in which dichlorosilane, SiH_2Cl_2, is reacted *in vacuo* with granular Li.[1] The second is the homogeneous chemical vapor deposition (HCVD) method using monosilane gas.[2,3] The last is the plasma chemical vapor deposition (PCVD) method using disilane (Si_2H_6) gas.[2–4] However, the alloys obtained by these three methods have only been studied by optical techniques and electron-spin-resonance (ESR) measurements. Moreover, the relationship between physical properties and the polysilane chain length n has not yet been clarified.

In this paper binary Si:H alloys containing many $(SiH_2)_n$ groups have been prepared by rf glow-discharge decomposition of disilane. The substrate temperature and the other glow-discharge parameters are systematically changed to obtain various kinds of Si:H alloys. Not only infrared-absorption, optical-gap, and photoluminescence measurements but also x-ray photoemission spectroscopy (XPS), ESR, dark and photoconductivity measurements are performed on the obtained alloys. The number of SiH_2 units that make up the $(SiH_2)_n$ chain, n, is estimated by the infrared-absorption peak shift for stretching vibrations. The relationship between the chain length n and macroscopic physical quantities are discussed. A microscopic structural model is also proposed for disilane-produced binary Si:H alloys containing many $(SiH_2)_n$ groups.

II. EXPERIMENT AND RESULTS

A. Experiment

The binary Si:H alloy film used in this study were prepared by rf glow discharge of disilane in a capacitively coupled reactor. The electrode diameter in the vacuum chamber is 12 cm, and the distance between electrodes is 4.5 cm. The rf power, total gas pressure, disilane-gas-flow rate and substrate temperature were 0.15—0.50 W, 0.10—0.30 Torr, 80—100 cm^3/min at STP (SCCM) and 220—440 K, respectively. The alloy was 1—2 μm thick and was deposited on glass, single-crystal silicon, and aluminum substrates except for the (220-K)-prepared specimen, which was deposited on a sapphire substrate. The films on the glass and sapphire substrates were observed by both optical absorption [(0.2—2.6 μm) (Ref. 4)] and photoluminescence. The films on single-crystal silicon substrates were observed by infrared absorption [(2.5—40 μm) (Ref. 4)], and by XPS. ESR measurements were performed on specimens deposited on aluminum and removed by dissolving the substrates in dilute acid.[5]

In order to measure the dark-conductivities and photoconductivities, aluminum was deposited onto alloy films on a glass substrate. The electrode pattern is interdigital, and its gap spacing is 0.5 mm. Such coplanar-type specimens were used for conductivity measurements, not only because the gap between electrodes is uniformly illuminated during photoconductivity measurements, but also because a high voltage can be applied due to its large gap spacing.[6] The current-voltage (I-V) data showed that the contact for the coplanar type specimens was nearly ohmic.

 ©1985 The American Physical Society

Conductivity measurements were performed by applying a high voltage (200 V) to ensure an ohmic contact.[6]

B. Optical-absorption measurements

Figure 1 shows the relationship between optical gap and substrate temperature during deposition. The optical gap was determined by $(\alpha\hbar\omega)^{1/2}$-vs-$\hbar\omega$, where α and $\hbar\omega$ are the absorption coefficient and the phonon energy, respectively. The specimens marked by an open circle were prepared under the following conditions: The rf power, the total gas pressure and the disilane-gas-flow rate were 0.2 W, 0.2 Torr, and 80 SCCM, respectively. Those marked by an open triangle had 0.5 W, 0.15 Torr, and 100 SCCM, respectively. The lower gas pressure with the higher gas-flow rate for the latter case indicates a higher pumping speed during glow discharge. As indicated in Fig. 1, optical gaps are sensitive to all glow-discharge parameters, particularly to substrate temperature. Optical gaps are monotonically increased with a decrease in the substrate temperature T_s during deposition in the range of $440 \gtrsim T_s \gtrsim 220$ K. By cooling the substrate down to 220 K, a 2.4-eV optical-gap value was obtained. This value is greater than those of previously obtained alloys prepared by monosilane and disilane glow discharge by 0.6 and 0.37 eV, respectively.[2,3]

Figure 2 shows the ratio of the peak infrared-absorption coefficient[4] near 845 cm^{-1} (wagging mode) to that near 890 cm^{-1} (bending mode) and it also shows the infrared-absorption-peak gravity center for the peak near 2100 cm^{-1} (stretching mode) as a function of the optical gap. The absorption bands near 845 and 890 cm^{-1} are sufficiently well resolved so that the peak absorption constant provides a good measure of the integrated absorption strength.[4,7] As indicated in Fig. 2, the optical gap is correlated to the ratio of $\alpha(845\ cm^{-1})/\alpha(890\ cm^{-1})$. It has been reported[7] that all SiH_2 groups contribute to the relatively strong absorption near 890 cm^{-1}, whereas only near-neighbor pairs of SiH_2 groups or large chain seg-

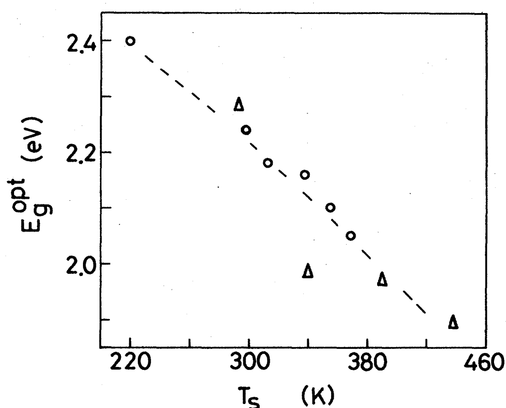

FIG. 1. Optical gap E_g^{opt} vs substrate temperature T_s, during deposition. The specimens marked by open circles were prepared under the conditions that rf power, total gas pressure, and disilane gas flow rate were 0.2 W, 0.2 Torr, and 80 SCCM, respectively. Those marked by open triangles were 0.5 W, 0.15 Torr, and 100 SCCM, respectively.

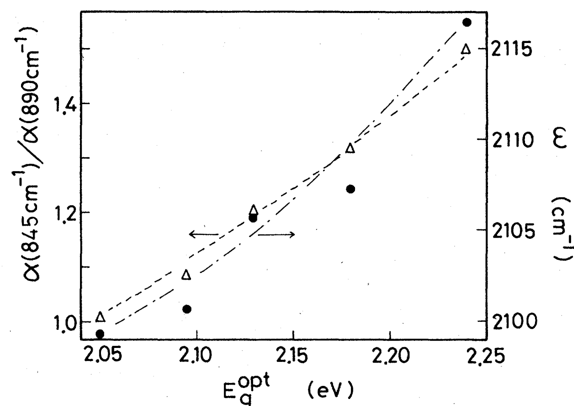

FIG. 2. Infrared-absorption coefficient ratio, $\alpha(845\ cm^{-1})/\alpha(890\ cm^{-1})$ and infrared-absorption peak gravity center ω for the peak near 2100 cm^{-1} vs optical gap E_g^{opt}.

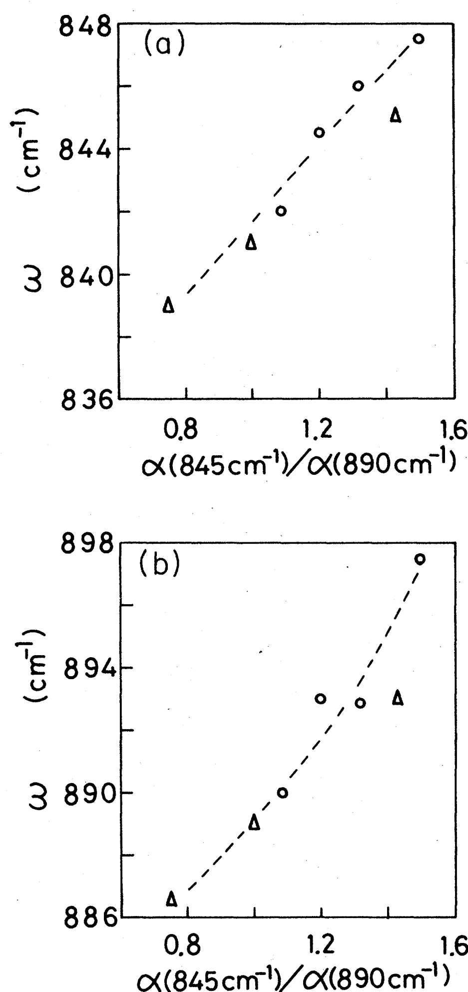

FIG. 3. Infrared-absorption wave-number shift for peaks near (a) 845 and (b) 890 cm^{-1} as a function of $\alpha(845\ cm^{-1})/\alpha(890\ cm^{-1})$.

ments, $(SiH_2)_n$, contribute to a strong absorption near 845 cm^{-1}. Therefore, the ratio of $\alpha(845\ cm^{-1})/\alpha(890\ cm^{-1})$ is considered to be a measure of the $(SiH_2)_n$ chain formation. From the relationship between $\alpha(845\ cm^{-1})/\alpha(890\ cm^{-1})$ and the optical gap in Fig. 2, it can be said that the optical-gap value is closely related to polysilane formation.

Not only infrared-absorption strength but also the absorption-peak wave number is correlated to polysilane formation or the optical band gap, as indicated in the $\omega - E_g^{opt}$ relation in Fig. 2. Similar absorption-peak shifts were also observed for the 845- and 890-cm^{-1} peaks (see Fig. 3) and the 640-cm^{-1} [$(SiH_2)_n$ rocking or isolated SiH_2 wagging mode] peak.[4] These wave-number shifts are not explained by SiH_3 formation, but by the increase in polysilane average chain length. This is because the higher frequency components relevant to SiH_3 groups, 862, 907, and 2140 cm^{-1}, are seldom included except for in an irregular specimen. The increase in the wave number is qualitatively explained by the increase in the electronegativity sum of the substituting groups, which is due to $(SiH_2)_n$ formation. Quantitative treatment of the peak shift as well as the above-mentioned irregular specimen will be discussed afterward.

Wide optical-gap ($\sim$2.1 eV) binary Si:H alloys have also been prepared from monosilane gas. The infrared-absorption spectrum for such wide optical-gap alloys showed the presence of $(SiH_2)_n$ groups. However, glow-discharge conditions for a wide optical-gap alloy derived from monosilane are highly restricted. Details will be published elsewhere.[8]

C. ESR and XPS measurements

Figure 4 shows the relationship between the substrate temperature during deposition and the spin defect density derived from the ESR signal. A similar relationship has been obtained by Wolford *et al.*[2,3] Both their and our results show the peak maximum at around $T_s \sim 360$ K.

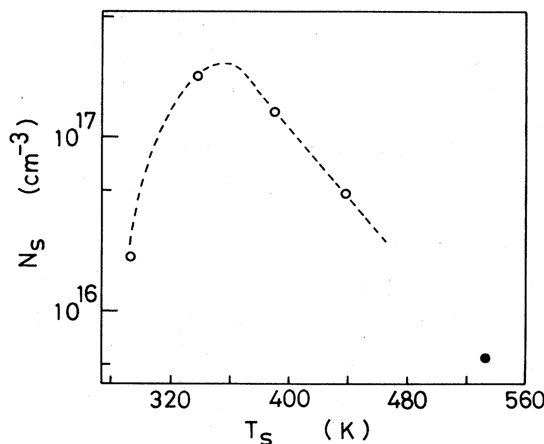

FIG. 4. ESR spin density N_s vs substrate temperature T_s, during deposition. The closed circle is for the (SiH_4)-prepared alloy.

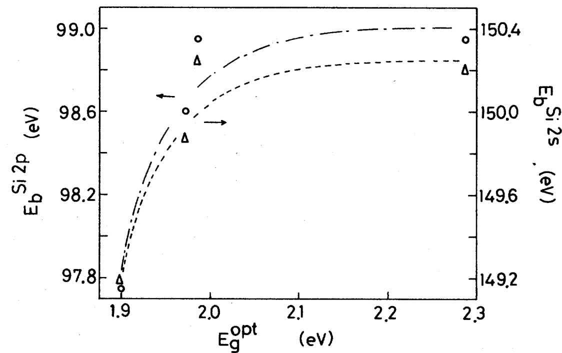

FIG. 5. Binding energies of Si 2s and 2p electrons measured by XPS vs optical gap, E_g^{opt}.

Below $T_s \sim 360$ K, the spin defect density decreases with a decrease in T_s.

Figure 5 shows the relationship between the optical gap and the binding energies of Si 2s and 2p electrons measured by x-ray photoemission spectroscopy (XPS). Below $E_g^{opt} \sim 2$ eV, both binding energies are drastically increased with an optical-gap increase. Above $E_g^{opt} \sim 2$ eV, the change in binding energy is small for both 2s and 2p electrons. It should be noted that a specimen having $E_g^{opt} \sim 2$ eV has been obtained at $T_s \sim 360$ K. This substrate temperature corresponds to the peak maximum of the N_s curve in Fig. 4. Details will be discussed afterward.

D. Electrical and photoluminescence measurements

Typical temperature dependence of dark conductivity is shown in Fig. 6. The optical gap was measured to be $\sim$2.4 eV for this specimen. The dark conductivity at room temperature is about 3×10^{-13} $(\Omega\,cm)^{-1}$. At low temperature, the change in dark conductivity is small.

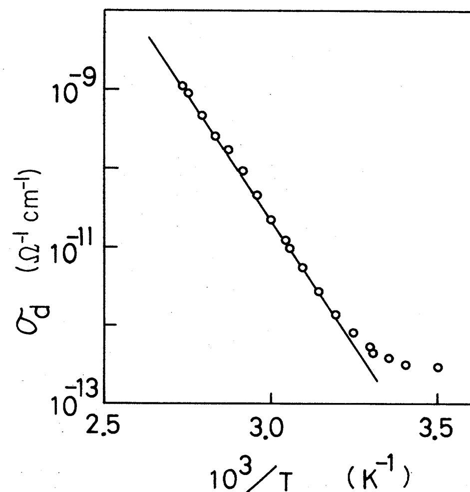

FIG. 6. Temperature dependence of dark conductivity (σ_d vs $10^3/T$) for a specimen whose optical gap is $\sim$2.4 eV.

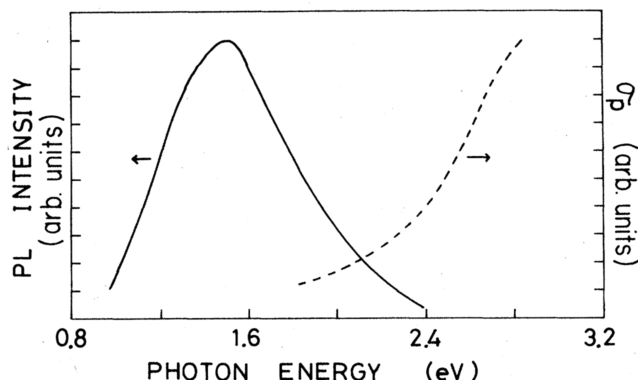

FIG. 7. Photoconductivity σ_p and photoluminescence (PL) vs photon energy. Measurements were performed at room temperature, and the specimen has an optical-gap value of ~2.3 eV.

However, conductivity increases markedly with an increase in the measurement temperature. At high temperature, there is an activation-type conductivity change, and its energy was evaluated to be 1.27 eV.

Figure 7 shows both photoconductivity dependence on incident photon energy and the photoluminescence spectrum for a specimen whose optical gap is ~2.3 eV. Both measurements were performed at room temperature. Photoconductivity is gradually increased with an increase in incident photon energy around its optical-gap energy. The photoluminescence spectrum has a relatively broad band and has high-energy components extending to the tail of the photoconductivity spectrum.

III. DISCUSSION

A. Estimation of polysilane chain length

The experimentally obtained infrared- (ir-) absorption peak shifts can be qualitatively explained by the electronegativity difference due to $(SiH_2)_n$ formation. Figure 8 shows the theoretical relationship between the effective electronegativity sum of substituting groups of $(SiH_2)_n$ and polysilane chain length n. In the calculation, the stability-ratio (SR) electronegativity scale is used, and it is assumed that there is an isolated $(SiH_2)_n$ group in a-Si network. By changing the terminal atoms of a $(SiH_2)_n$ group, another model, H-$(SiH_2)_n$-H, can also be considered. However, the latter model is unrealistic, because there should be higher silane molecules embedded in the a-Si:H network with a small value for n. Moreover, the latter model is inconsistent with the ir data, in which the higher frequency component[7] relevant to the terminal SiH_3 groups is not contained. Therefore, the present assumption relevant to terminal atoms [$\equiv Si-(SiH_2)_n-Si\equiv$] is reasonable. For $n \geq 3$, all SiH_2 groups in a $(SiH_2)_n$ chain do not necessarily have the same value for the electronegativity sum. Accordingly, first the sum of the substituting groups was calculated for each SiH_2 unit in a $(SiH_2)_n$ chain. Then, they were averaged to obtain the effective electronegativity sum. The scale of the right vertical axis in Fig. 8 is the corresponding wave number for stretching vibrations, which has been obtained by the linear relationship between the electronegativity sum and the wave number.[7]

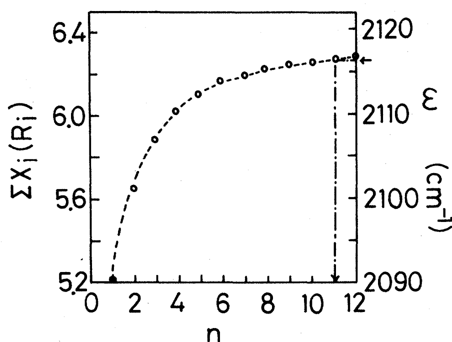

FIG. 8. Theoretical relationship between the effective electronegativity sum $\sum X_i(R_i)$ of substituting groups of $(SiH_2)_n$ and polysilane chain length n. The scale of the right vertical axis is the corresponding wave number ω for stretching vibrations, which has been obtained by the linear relationship between the electronegativity sum and the wave number in Ref. 7.

From the results in Fig. 8, the wave-number shifts in Figs. 2 and 3 and Ref. 4 can be explained qualitatively by the increase in the average chain length of $(SiH_2)_n$. For the largest wave number value for stretching vibrations in Fig. 2, 2116.5 cm^{-1}, the polysilane chain length is estimated to be 11. The corresponding specimen has been prepared at $T_s \sim 300$ K. Therefore, it can be said that the average polysilane chain length evaluated by ir data for a (300-K)-prepared alloy is about 11.

Both foreign atoms and neighboring $(SiH_2)_n$ chains may cause a shift in the vibrational frequencies which are utilized to obtain the n value. However, the latter effect is small because of the nondirect effect. The effect of neighboring polysilane chains occurs through more than one Si atom, and the electronegativity effect of a SiH_2 group is drastically reduced in the second-neighbor groups (the third-neighbor Si atoms from the hydrogen atom of a SiH_2 group).[9]

B. Details of the ~640-cm^{-1} peak in the infrared-absorption spectrum

The infrared-absorption peak near 640 cm^{-1} had the following two distinctive points.[4] One is its large width of half the maximum, and its nonsymmetrical shape. The other is a nonlinear shift in its peak gravity center with α(845 cm^{-1})/α(890 cm^{-1}) (see Fig. 3 of Ref. 4). These phenomena can qualitatively be explained by introducing two different modes near 640 cm^{-1}.

Figure 9 shows the infrared-absorption spectrum for a specimen prepared at a relatively high temperature, $T_s \sim 360$ K. It should be noted that absorption near 640 cm^{-1} consists of two peaks. Table I shows the previously calculated and experimentally obtained vibrational frequencies for wagging and rocking models.[10] Although the calculated value for the isolated SiH_2 wagging mode is different from that for the $(SiH_2)_n$ ($n \geq 2$) rocking mode,

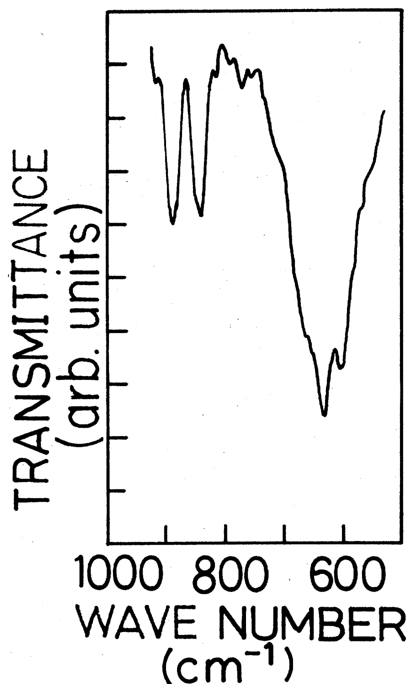

FIG. 9. Infrared-absorption spectrum for a specimen prepared at relative high temperature, $T_s \sim 360$ K.

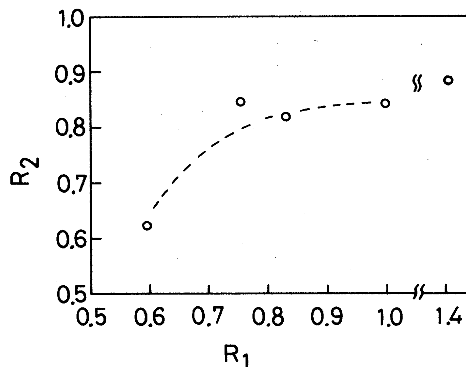

FIG. 10. Infrared-absorption coefficient ratio, $R_1 = \alpha(845\ \mathrm{cm}^{-1})/\alpha(890\ \mathrm{cm}^{-1})$, vs infrared-absorption coefficient ratio for the doublet near 640 cm^{-1}, $R_2 = \alpha(\sim 600\ \mathrm{cm}^{-1})/\alpha(\sim 640\ \mathrm{cm}^{-1})$.

these two modes were experimentally indistinguishable. The present doublet near 640 cm^{-1} is assigned to be a $(SiH_2)_n$ rocking mode for a lower frequency small peak and an isolated SiH_2 wagging mode for a higher frequency large peak. In fact, the absorption-coefficient ratio for the doublet near 640 cm^{-1}, $\alpha(\sim 600\ \mathrm{cm}^{-1})/\alpha(\sim 640\ \mathrm{cm}^{-1})$, is positively correlated to $\alpha(845\ \mathrm{cm}^{-1})/\alpha(890\ \mathrm{cm}^{-1})$, as shown in Fig. 10. The data show that the lower frequency component of the doublet near 640 cm^{-1} is related to $(SiH_2)_n$ groups.

The nonlinear shift[4] in the ~ 640 cm^{-1} absorption-peak gravity center with $\alpha(845\ \mathrm{cm}^{-1})/\alpha(890\ \mathrm{cm}^{-1})$ is explained as follows. That is, the $(SiH_2)_n$ rocking frequency is continuously increased with an increase in the polysilane chain length, whereas the isolated SiH_2 wagging frequency is essentially unchanged, because wagging frequency jumps to ~ 845 cm^{-1} due to $(SiH_2)_n$ formation.[7] At a relatively small $\alpha(845\ \mathrm{cm}^{-1})/\alpha(890\ \mathrm{cm}^{-1})$, an increase in $\alpha(845\ \mathrm{cm}^{-1})/\alpha(890\ \mathrm{cm}^{-1})$ causes both a frequency shift and an increase in absorption strength for the lower frequency component. These two phenomena have opposite effects on the total frequency shift. Therefore, the frequency shift is relatively small for a small $\alpha(845\ \mathrm{cm}^{-1})/\alpha(890\ \mathrm{cm}^{-1})$. On the other hand, for a large $\alpha(845\ \mathrm{cm}^{-1})/\alpha(890\ \mathrm{cm}^{-1})$, isolated SiH_2 groups are seldom included in the alloy. Therefore, this absorption peak near 640 cm^{-1} is mostly caused by the $(SiH_2)_n$ rocking mode. In this case, the increase in absorption strength causes a direct increase in the vibrational frequency. The above discussion explains the frequency shift for the ~ 640 cm^{-1} peak in Ref. 4.

TABLE I. Previously calculated and experimentally obtained vibrational frequencies for wagging and rocking modes (Ref. 10). Units are cm^{-1}.

	SiH_2		$(SiH_2)_n$	
Mode	Calc.	Expt.	Calc.	Expt.
Wagging	651	630	821	845
Rocking	501		538	630

From Fig. 8 and the stretching frequency (not shown for this mode in Fig. 9), the average chain length for the specimen shown in Fig. 9 is estimated to be $n = 1$–2. This is reasonable because the alloy corresponding to Fig. 9 should contain both isolated SiH_2 and $(SiH_2)_n$ $(n \geq 2)$ groups.

C. On qualitative changes in ESR and XPS data

As shown in the previous figures (Figs. 1, 4, and 5), the optical gap is monotonically increased with a decrease in T_s, whereas ESR and XPS data show a critical change at around $T_s \sim 360$ K. This T_s value corresponds to a $(SiH_2)_n$ chain length of $n = 1$–2. That is, $(SiH_2)_n$ $(n \geq 2)$ groups are formed below ~ 360 K, and only isolated SiH_2 groups are formed above ~ 360 K. Therefore, the results in Figs. 4 and 5 indicate that polysilane $(SiH_2)_n$ $(n \geq 2)$ formation causes a qualitative change in these physical quantities.

The decrease in ESR spin density below ~ 360 K may come from a reduction of the restriction force that relates to alloy network construction due to $(SiH_2)_n$ formation. The ESR spin density in relation to the alloy growth mechanism has been discussed elsewhere.[5]

The relationship between the binding energies of Si $2s$ and $2p$ electrons and substrate temperature is also revealed to be nonlinear as in Fig. 5. These nonlinear relationships are not clear when hydrogen atoms only affect the binding energies of the nearest-neighbor Si atoms equivalently, because the hydrogen content increases linearly with a decrease in the substrate temperature.[5] Therefore, the present nonlinear relationship between

binding energies and substrate temperature, or between binding energies and the optical gap, may be explained by the hydrogen effect on the second-neighbor Si atoms or the nonequivalent effect of hydrogen atoms on the nearest-neighbor Si atom due to $(SiH_2)_n$ formation. The former effect is consistent with the previous discussion of the wave-number shift due to electronegativity difference, in which hydrogen atoms not only affect the nearest-neighbor Si atom but also the second-neighbor Si atoms (strictly speaking, all of the other atoms).

D. Microscopic structural model

A microscopic structural model can be constructed on the basis of data for polysilane chain length and hydrogen content.[5] Figure 11 shows microscopic models for the present alloy. The model is not for $\bar{n} \sim 11$ ($T_s \sim 300$ K) but for $\bar{n} = 4$–6 ($T_s \sim$ 320 K). However, they are the same in basic features. That is, the alloys consist of polysilane $(SiH_2)_n$ chains and very small silicon clusters. The existence of the latter is determined from evidence that the alloy does not have an ideal stoichiometry, i.e., (Si atoms):(H atoms) not equal to 1:2 (or, the hydrogen content is less than 66.7%).[5] Even if hydrogen content is less than 66.7%, it is better to say that the present alloy is not just a simple silicon-based alloy, but rather a SiH_2- or $(SiH_2)_n$-based alloy.

The model is, at a glance, inconsistent with optical- (visible) absorption measurements, in which low-energy photons ($\lambda \sim 0.5$ μm) are only absorbed by the present alloy to a limited extent. It is curious that the small silicon clusters (*a*-Si phase) in the model do not absorb relatively-low-energy photons. The reason is considered to be as follows. Silicon atoms in very small clusters are not the same as those in a conventional *a*-Si network, and may be affected by the strong effect of the hydrogen atoms in neighboring $(SiH_2)_n$ chains. In this case, the local density of states for the affected silicon atoms may be changed to widen the band gap. This relatively long-range (farther than the second neighbor) effect of hydrogen atoms in a polysilane chain is supported by the previously stated electronegativity effect and the discussion relevant to nonlinear XPS data. Therefore, the present model is not actually inconsistent with optical- (visible) absorption measurements.

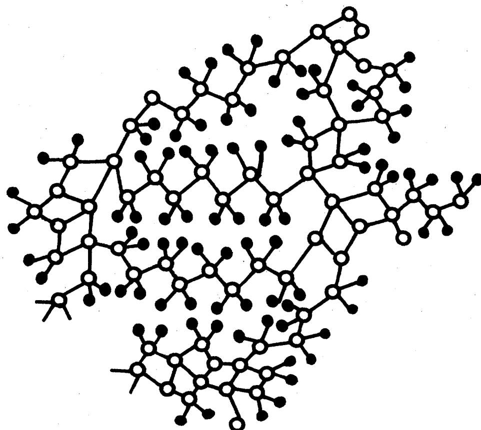

FIG. 11. Microscopic structural model for the present Si:H alloy. Open and closed circles indicate silicon and hydrogen atoms, respectively. (In the real alloy, both *cis* and *trans* conformations are randomly included.)

A final discussion of the microscopic model is relevant to *cis-trans* configurations of the $(SiH_2)_n$ structure. As stated previously, one specimen showed an irregular ir spectrum in which higher frequency components ($\sim$907 cm^{-1}) are included. This specimen corresponds to the open triangle plotted on the right-hand side of Fig. 3. The plot does not fit the curve obtained from the other six plots. One possible reason for this irregularity is the difference in the microscopic structural configuration. Lucovksy[10] has suggested that the higher frequency pair at 862–907 cm^{-1} is due to a polymer with a higher degree of order, as for example in a *trans* conformation. The irregular specimen (this does not mean an irregular configuration, but means an irregular plot) may contain many *trans*-$(SiH_2)_n$ groups.

E. Band structure

Finally, the band structure of the present Si:H alloy will be discussed. Although, the density-of-states (DOS) distribution for the present alloy is experimentally unclear, a theoretical DOS calculation has been performed for an ideal polysilane.[11] According to the calculation, the energy gap increases with an increasing H content, predicting a maximum attainable gap of $\sim$3.0 eV. The present maximum optical gap is $\sim$2.4 eV, and is smaller than that of an ideal polysilane by about 0.6 eV. The following two reasons may be considered for the discrepancy. One is the present alloy's hydrogen content of less than 66.7%. This may affect the band structure through the appearance of the states in the ideal gap. The other reason is band-gap narrowing due to tail states arising from disorder in the real alloy. The broad-band photoluminescence and the long tail in the photoconductivity spectrum in Fig. 7 may support the existence of the broad tail states.

The activation energy of 1.27 eV shown in Fig. 6 indicates the approximate position of the Fermi level measured from the mobility edge E_c (Ref. 12) (when E_c exists). This large activation energy may come from a localization of states near the optical-gap edge on the conduction-band side.[13] However, more detailed experiments are necessary to construct an accurate band diagram for the present alloy.

IV. SUMMARY AND CONCLUSION

Binary Si:H alloys containing many polysilane $(SiH_2)_n$ groups have been prepared by rf-glow-discharge decomposition of disilane in a capacitively coupled reactor. The optical gaps are monotonically increased with a decrease in the substrate temperature T_s during deposition in the range of $440 \gtrsim T_s \gtrsim 220$ K. The maximum optical-gap value obtained is 2.4 eV. This value is comparable with that for an HCVD-prepared alloy. The increase in the op-

tical gap is closely related to the infrared-absorption strength for the $\sim 845\ cm^{-1}$ peak, which is due to $(SiH_2)_n$ wagging vibrations. The infrared-absorption wave number increases slightly with an increase in polysilane formation. The shift in the infrared-absorption wave number can be explained by the effective electronegativity increase due to $(SiH_2)_n$ formation. The polysilane chain length n can be estimated by the stretching wave-number shift and is evaluated to be $n \sim 11$ for the alloy prepared at $T_s \sim 300$ K. The microscopic structural model can be constructed on the basis of data for polysilane chain length and hydrogen content. The extraordinary nonlinear wave-number shift for the $\sim 640\ cm^{-1}$ peak is explained by the introduction of two different vibrational modes. The binding energies of Si inner electrons estimated from XPS measurements and ESR spin density do not show a monotonical change with a change in T_s, but show a critical change at around 360 K. This T_s value corresponds to $n = 1-2$, indicating that $(SiH_2)_n$ ($n \geq 2$) group formation causes a qualitative change in XPS and ESR data. The dark conductivity of a wide optical-gap (~ 2.4 eV) alloy is smaller than that of conventional *a*-Si:H by about three orders of magnitude. Although the band structure of the binary Si:H alloy containing many $(SiH_2)_n$ groups has not yet been clarified, the present electrical measurements suggest both the existence of broad tail states and the localization of the states which determine the optical gap. More detailed experiments should be performed to clarify the band structure of a wide optical-gap Si:H alloy containing $(SiH_2)_n$ groups.

[1]P. John, I. M. Odeh, M. J. K. Thomas, and J. I. B. Wilson, J. Phys. (Paris) Colloq. Suppl. 10 **42**, C4-651 (1981).

[2]D. J. Wolford, B. A. Scott, J. A. Reimer, and J. A. Bradley, in *16th International Conference on the Physics of Semiconductors, Montpellier, 1982* [Physica **117&118B**, 920 (1983)].

[3]D. J. Wolford, J. A. Reimer, and B. A. Scott, Appl. Phys. Lett. **42**, 369 (1983).

[4]S. Furukawa and N. Matsumoto, Solid State Commun. **48**, 539 (1983).

[5]B. A. Scott, J. A. Reimer, and P. A. Longeway, J. Appl. Phys. **54**, 6853 (1983).

[6]S. Furukawa, T. Kagawa, and N. Matsumoto, Solid State Commun. **44**, 927 (1982).

[7]G. Lucovsky, R. J. Nemanich, and J. C. Knights, Phys. Rev. B **19**, 2064 (1979).

[8]S. Furukawa and N. Matsumoto J. Non-Cryst. Solids (to be published).

[9]W. B. Pollard and G. Lukovsky, Phys. Rev. B **26**, 3172 (1982).

[10]G. Lucovsky, *Fundamental Physics of Amorphous Semiconductors*, edited by F. Yonezawa (Springer, Berlin, 1981).

[11]D. C. Allan and J. D. Joannopoulos, Phys. Rev. Lett. **44**, 43 (1980).

[12]S. Furukawa and N. Matsumoto, Phys. Rev. B **27**, 4955 (1983).

[13]S. Furukawa and N. Matsumoto, Solid State Commun. **51**, 833 (1984).